World Conference on Timber Engineering Oslo 2023

SEISMIC FRAGILITY OF A NEW MASS TIMBER-STEEL HYBRID BUILDING SYSTEM EQUIPPED WITH CLT FLOOR DIAPHRAGMS

Chaoyue Zhang[1], Cristiano Loss[2]

ABSTRACT: An essential step in analysing a Seismic Force-Resisting System (SFRS) is to ascertain how lateral loads distribute within the structure in-between horizontal systems, such as roof and floor diaphragms, and vertical members, such as shear walls and bracings. Clear identification of load paths requires a proper assessment of the in-plane stiffness of floor diaphragms. Nevertheless, in the context of designing SFRS with diaphragms made of wood, neither comprehensive code provisions nor accurate computational methods exist to account for its in-plane flexibility. This shortage of knowledge becomes even more obvious if compared to the common reinforced concrete flooring systems. To investigate influences of the actual in-plane stiffness of diaphragms on the global response of the SFRS, this research performs incremental dynamic analysis (IDA) on a new mass timber-steel hybrid building system via the OpenSees platform and compares its collapse fragility to that of an ideal building model with rigid diaphragms. The SFRS of hybrid building entails concentrically X-braced steel frames, whose nonlinear responses are explicitly simulated, including global buckling, tensile yielding, and post-buckling behaviours. Overall, the fragility analysis concluded that the adoption of the proposed hybrid floor system, with the reinforcement of panel-to-panel connections that contributes to sufficient in-plane stiffness, can facilitate a comparable seismic performance as the building with the fully rigid diaphragm.

KEYWORDS: Mass timber-steel hybrid building, In-plane diaphragm flexibility, IDA, OpenSees modelling

1 INTRODUCTION

1.1 HYBRID MASS TIMBER CONSTRUCTION

Hybrid mass timber construction refers to structural assemblies that combine engineered wood products, such as cross-laminated timber (CLT), with concrete and/or steel. By leveraging the prefabrication method, massive production off-site and speedy assembly on-site of large timber members can be readily attained. With previous research mostly focusing on the lateral behaviour of CLT shear walls and bracing systems, attention is shifting to high-performance earthquake-resistant systems equipped with CLT floor diaphragms.

1.2 IN-PLANE DIAPHRAGM FLEXIBILITY

Floor diaphragms are designed to resist gravity loads and transmit lateral loads to adjoining vertical members of the Seismic Force-Resisting System (SFRS). As a convention in seismic design, rigid diaphragms distribute applied lateral shear forces by the relative rigidity of the SFRS, whereas flexible diaphragms distribute forces based on tributary area. Consequently, to properly assess diaphragm flexibility is imperative to quantify the lateral force demands and, as such, produce economic proportion and sizing of structural members of an SFRS. In terms of the dynamic response, the diaphragm's flexibility plays a pivotal role in affecting the global dynamic behaviour of buildings as well as the local distribution of inertia forces, shears, and bending moments along the edges of the diaphragm [1]. However, most building codes lack the criteria for specifying the actual in-plane stiffness of wood and mass timber diaphragms by explicitly specifying reduction factors used for seismic design. Practitioners must confront inevitable challenges when attempting to incorporate mass timber floor assemblies into a high-performance hybrid building system.

2 HYBRID TIMBER-STEEL BUILDING

2.1 DESCRIPTION OF THE BUILDING

Figure 1 shows the architectural view of the 4-story timber-steel building prototype that entails a Special Concentrically Braced Frame (SCBF) with repeatable modules of innovative CLT-steel floor diaphragms.

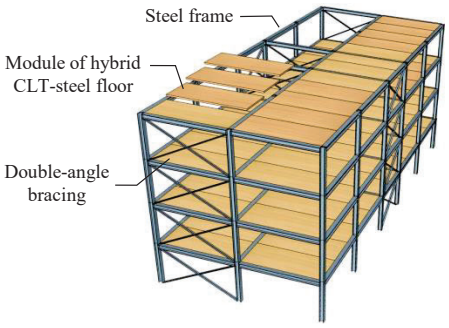

Figure 1: *Mass timber-steel hybrid building archetype*

[1] Chaoyue Zhang, Sustainable Engineered Structural Solutions Laboratory, The University of British Columbia, Canada, chaoyuez@mail.ubc.ca

[2] Cristiano Loss, Sustainable Engineered Structural Solutions Laboratory, The University of British Columbia, Canada, cristiano.loss@ubc.ca

https://doi.org/10.52202/069179-0423

The building has a 28.5 m long by 12 m wide footprint, with a 3.2 m inter-story height. Structural novelties of the hybrid floor modules are attributed to the composite action engaged between the CLT panels and steel beams. From the structural perspective, the high strength-to-weight ratio of CLT panels can impart the overall hybrid system with sufficient in-plane stability when subjected to horizontal forces. When subjected to severe earthquake excitations, the lightness of mass timber-based floors can effectively reduce the demands of the induced inertia forces acting upon each story.

2.2 DESIGN CONSIDERATIONS

The proposed CLT-steel hybrid building archetype was designed for residential usage, and located in Bucchianico, Chieti, Italy [2]. For the gravity design, a specified dead load (G_2) of 3 kN/m^2 plus a live load (Q) of 2 kN/m^{2}was adopted, factored by 0.3 (Ψ_2) according to the load combination parameters defined in the Italian Building Code [3] for multi-story residential buildings. The estimated total gravity load for stories 1 to 3 was 3.6 kN/m^2; the total gravity load for story 4 was 3 kN/m^2. The seismic design of the hybrid building followed the equivalent linear elastic force procedure of Eurocode 8 [4] with reference to "other" structure types. The design response spectrum was drawn given the soil class type C, typographical category type "t1", and a building life span of 50 years. The code-based fundamental period of the building was estimated at 0.34 seconds, based on the total height of the superstructure. Considering the local seismic hazard having a 10% probability of exceedance, corresponding to the life safety performance level defined in Eurocode (2004), the design base shear force for the 4-story building archetype was calculated as 1200 kN after applying a reduction factor *q* of 4 to account for system overstrength and ductility of typical braced steel frame structures.

Table 1: Selection of steel elements

Elements	Sections	Steel
Beams	IPE 360	S355
	IPE 300	S355
	IPE 220	S275
Columns	HEB 220	S275
	HEB 300	S275
	HEB 280	S275
	HEB 220	S275
Braces	2L 110X70X12	S275
	2L 100X65X10	S275
	2L 60X60X8	S275

The steel structs, including beams, girders, columns, and braces, of the SCBF employed parallel flange I-shaped (IPE), wide flange H-shaped (HEB), and L-formed hot rolled profiles with steel in S275 and S355 strength class [4], respectively. Table 1 lists the selected cross sections and materials of beams, columns, and braces. Notice that a stockier section (2L 110X70X12) is used for braces at the first and second story considering potential greater demands of seismic force and deformation at the lower stories during earthquake ground shakings. The SFRS of the four-story building adopted dissipative SCBFs, with steel struts and connections sized and detailed to enforce major inelastic deformation of bracing diagonals and maintain elastic deformation of beams and columns. Properly capacity-designed SFRSs provide the building with outstanding lateral strength and stiffness. Considering large and infrequent seismic events, the compressive buckling and yielding tensile behaviour of the bracing elements can offer incredible ductile deformability to accommodate the induced large inelastic drift demands and assure the satisfaction of intended performance levels. The beam-to-column joints of the unbraced frame consisted of shear tabs, while the beam-to-column-brace joints of the braced frame were reinforced by welding gusset plates.

2.3 HYBRID CLT-STEEL FLOOR DIAPHRAGMS

Figure 2 details the key components of the innovative hybrid CLT-steel floor module, which can be demounted into two main parts: the CLT panel and two customized cold-formed U-shaped beams. The 85 mm thick CLT panel of one floor module is 2.4 m in width and 5.83 m in length. Two U-shaped steel beams that attach to the CLT panel are 5.815 m long and are manufactured by 4 mm thick S355 steel sheets [4]. Moreover, the four 140 mm wide perforated steel plates at each end of the U-shaped beam are bounded to the CLT panel by pouring an epoxy-based resin into precut slots (A-A). In the middle section of the U-shape beam (B-B), 80 mm long full-threaded self-tapping screws (STSs) are driven into predrilled holes at a spacing of 500 mm to connect with the panel.

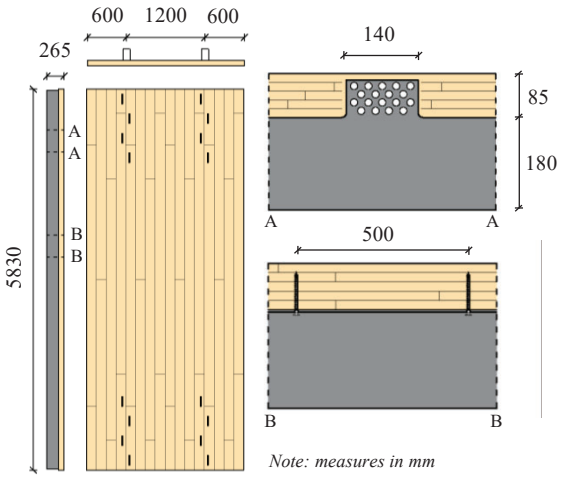

Figure 2: *Hybrid CLT-steel floor diaphragm module*

Each prefabricated hybrid floor module is installed into the braced steel frames by bolting special steel links to the ends of the U-shaped beams. Figure 3a shows the configuration of the beam-to-beam special links. Multiple pairs of STSs oriented at the designated angle, as shown

https://doi.org/10.52202/069179-0423

in Figure 3b, are used to fasten the edges of the CLT panels in order to create a continuous slab. Application of those special steel links between the steel frame and hybrid floor modules not only accommodates potential structural misalignment or imperfections but also allows for rapid replacement of any damaged components after major earthquake events. Furthermore, the prefabricated floor modules can greatly accelerate on-site assembly and, as such, effectively save total fabrication time and labour costs. Large-scale implementation of the proposed hybrid system can conceivably leverage most prefabrication techniques.

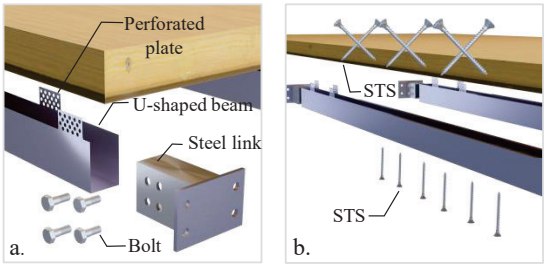

Figure 3: *Beam-to-beam and panel-to-panel connections*

3 NUMERICAL INVESTIGATION

3.1 MODEL OF FLOOR DIAPHRAGM

Finite-element (FE) sub-modelling approach aims to reproduce the in-plane shear stiffness and failure mechanisms recorded in the full-scale experiment of the hybrid CLT-steel floor diaphragm performed by [5]. Figure 4 shows features of the constructed test specimen assembled by staggering the hybrid prefabricated CLT-steel floor modules. The dimensions of the specimen were 6 m in width and 12 m in length. The location of the applied in-plane shear load, *F*, is also annotated in Figure 4. To highlight the contributions of the panel-to-panel connections to the in-plane shear stiffness of the diaphragm, to tests were performed on the same floor specimen by installing and removing the STSs at the edges of the CLT panels.

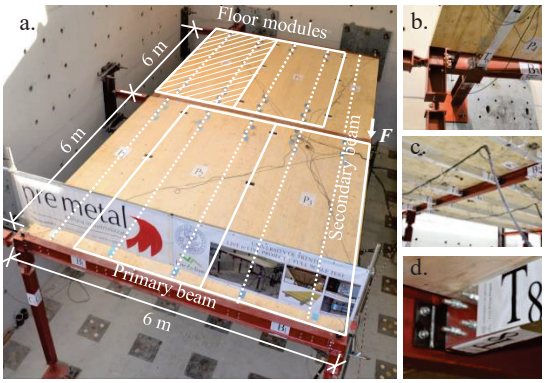

Figure 4: *Floor subassembly of the full-scale in-plane test*

3.1.1 Component modelling

It has been shown that the ductile and dissipative behaviour of the connections governs the performance of the tested hybrid steel-timber floor diaphragm. No damage in the 5-layer CLT panels was observed after each of the three in-plane shear tests performed. In OpenSees [6], CLT is thus modelled by the *ShellMIT4* element with the *PlateFiber* section and *ElasticOrthotropic* material. According to Loss and Frangi [5], the observed deterioration mechanism demonstrated superior composite actions between timber and steel elements together with weak component joints. Significant ductile deformation was found to concentrate at the beam-to-beam connections. The local shear-tension breakage of the bolts that fastened the outstanding flanges of the steel link outlined the ultimate failure point of the floor system. To replicate the distinctive nonlinear behaviour of the beam-to-beam connection, the numerical representation of the steel link consists of four parts linked in series: (i) a *ZeroLength* element that represents the bolt contact gap, (ii) a short hollow tube that slots in the U-shaped beam, (iii) outstanding flanges that are welded to the hollow tube, and (iv) bolts connected to the primary beam, as shown in Figure 5b. Both the steel tube with hollow section and the flange segment with rectangular section are modelled by the *forceBeamColumn* element with discretized fibre section and *Steel02* material. The two ends of the flange are connected to the primary beam by two nonlinear axial springs using the *ZeroLength* element. Figure 5a illustrates the boundary restraints of the floor subassembly, which are modelled as rollers with translative DOFs constrained only.

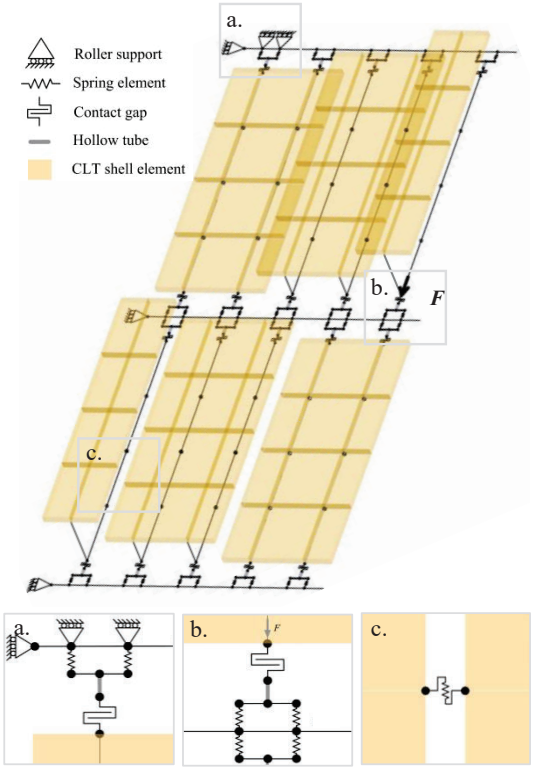

Figure 5: *OpenSees model of the hybrid floor subassembly*

In addition, under seismic actions, the induced in-plane shear transferred between CLT panels could place significant slip demands on the STSs. Datasets retrieved from cyclic tests of panel-to-panel STS connections performed by Loss et al. [7] were used to represent their hysteretic behaviour. In OpenSees, the *Pinching4* material was used to simulate the strength and stiffness degradation of the pane-to-panel connections in the in-plane shear direction.

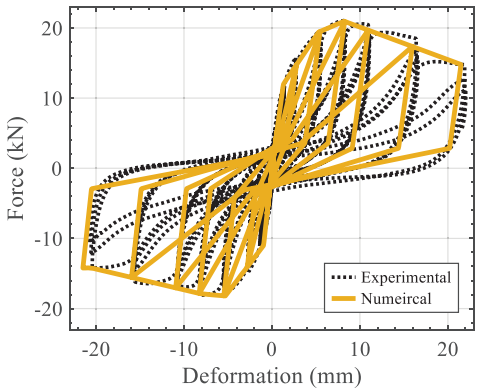

Figure 6: *Calibrated behavior of panel-to-panel connections*

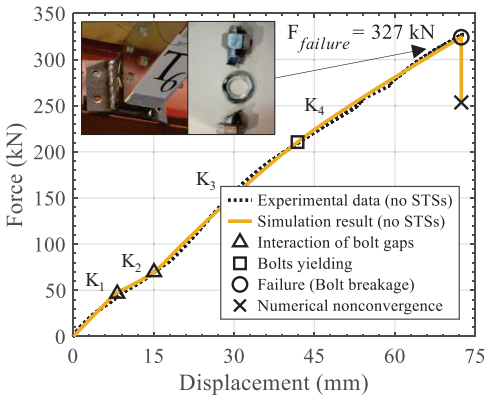

Figure 7: Validated response of floor model without STSs

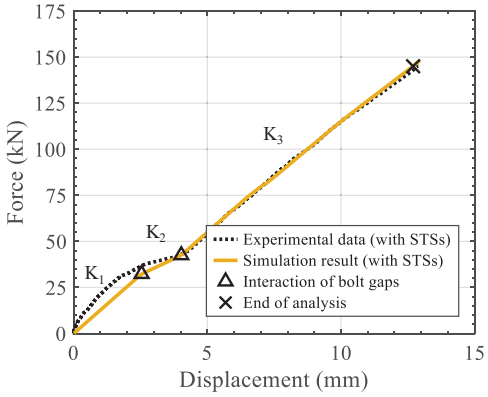

Figure 8: Validated response of floor model with STSs

Figure 6 shows the calibrated hysteretic response of the STS, which is characterized by a severe loss in stiffness in reloading. Such known pinching behaviour is not uncommon for steel mechanical connectors embedded in timber due to the crushing the wood fibers underneath the connector surface. Consequently, the calibrated material was assigned to the nonlinear translational spring using a *ZeroLength* element, as shown in Figure 5c. For simulating the test specimen without the panel-to-panel connections, the physical contact between panels was idealized by embedding the *ElasticPPGap* material into the *ZeroLength* element. High compressive stiffness and strength with zero tensile resistance were added to the material to prevent mutual penetration of CLT shell elements.

3.1.2 Model validation

Model validation of the CLT-steel hybrid floor diaphragm subassembly was accomplished by simulating T_2 and T_3 in-plane shear tests published in [5]. For the specimen subjected to a destructive monotonic test (T_3), the CLT panels were not tied together with STSs. Figure 7 plots the well-matched simulated results of the numerical model versus the experimental data, with a maximum error of about 13% in values in terms of in-plane stiffness K_2. The initial drop of stiffness, from K_1 to K_2, when displacement reaches about 7 mm, is attributed to the interaction of bolt-hole gaps between the hollow steel tube and the U-shaped beam. After the gap is closed, the in-plane stiffness restores to the initial level before the beam-to-beam connections bolts yield, which signifies a further small reduction of the overall shear stiffness. When the applied in-plane load increases up to approximately 327 kN, the deformation of the beam-to-beam connections reaches the maximum, which results in the breakage of bolts under combined effects of shear and tension, as annotated by the detached flange in Figure 7. In the numerical model, only the axial tensile resistance of the bolt is considered, and its ultimate capacity is ascertained by calibrating to the test result by warping *Steel02* material with *fatigue* material, which can trigger failure based on a predefined maximum deformation.

Figure 8 shows the simulation results of T_2 test, including the panel-to-panel connections. The simulated K_1 and K_2 have a relatively large deviation from the measured in-plane stiffness with a maximum error beyond 30%. It should be noted that the results of the original cyclic test program (T_2) published in [5] did not display a distinctive hysteretic or deteriorated response as for the in-plane shear force and displacement relationship. A marginal reduction in stiffness occurred during the unloading phase with a maximum relative residual deformation equal to 2 mm only. This slight offset from the original position was mostly due to the friction between the steel-to-steel surfaces of the beam-to-beam connections. No degradation of stiffness and strength was observed during the reloading phase. Therefore, the numerical model of the hybrid floor subassembly, inclusive of the panel-to-panel connections, was shown to capture the overall behaviour of the system and its members.

https://doi.org/10.52202/069179-0423

3.2 MODEL OF STEEL FRAME

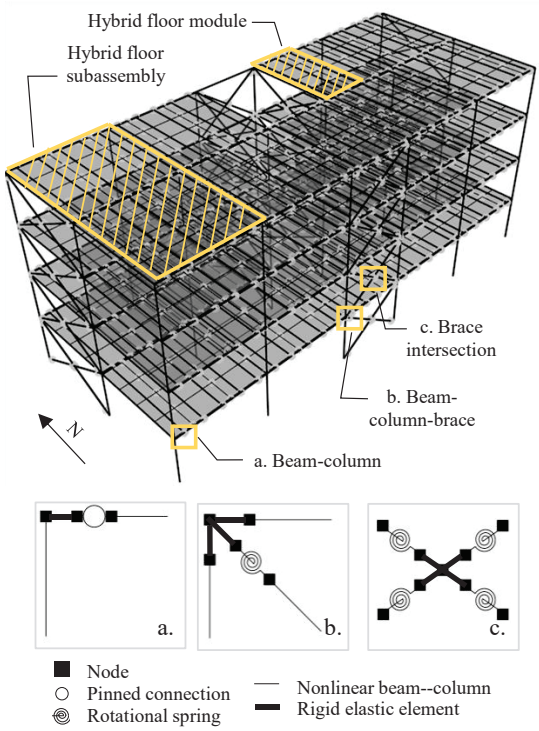

Figure 9: *OpenSees model of the hybrid building archetype*

To accurately predict the building's seismic performance throughout varying limit states, a reliable FE model should explicitly capture critical nonlinear deterioration modes and failure mechanisms of structural components. Numerical models of steel structs of the braced frame implemented in this paper, such as brace, beam, and column, take advantage of the state-of-art nonlinear frame elements in OpenSees [8]. Such frame element was created to explicitly simulate the nonlinear material response due to the post-yielding behaviours of the steel members, such as strain hardening. Being a fibre-type model, it applies the distributed plasticity theorem through numerical integrations of stress resultants over discretized sections along the member length.

3.2.1 Component modelling

Characteristic deterioration modes of braces include buckling in compression, yielding in tension, and post-buckling behaviour. In this work, multiple *forceBeamColumn* elements with finely meshed fibre cross sections were used to produce those highly nonlinear responses, as suggested by Uriz and Mahin [9]. This verified method applies to a range of cross-section shapes of braces, such as hollow circular, hollow square, I wide flange, and double angles. To account for geometric nonlinearities when brace buckles with substantial axial deformation under compression, the *forceBeamColumn* elements were assigned with *Corotational* transformation with exact nonlinear transformation of element displacement and forces between the global and local coordinate systems [10].

Large rotational and axial forces concentrated in bracing members also attract great nonlinearities to their adjacent components. Hsiao et al. [11] indicated that local yielding in beams and columns was significant based on previous experiments. To simulate the nonlinear behaviour of the beams and columns, the *dispBeamColumn* element was used.

Connections between beams and columns of unbraced bays were designed using shear tabs. The actual bending stiffness of shear tab connections along the strong axis of beams does not evidently contribute to the moment resistance of beam-to-column joints. Hence, it was simplified as a pin connection plus a short-length element equal to the half depth of the column, as shown in Figure 9a. The idealized pin connection was modelled by implementing the *EqualDOF* constraint with the designated rotational degree-of-freedom (DOF) released. For the braced bays, the presence of gusset plates provides additional reinforcement to the beam-to-column connection and, meanwhile, serves as the critical boundary condition for the brace. Yoo [12] suggested that the out-of-plane rotational stiffness of the gusset plate plays an important role in affecting brace buckling and post-bulking behaviours, given the considerable rotation demands. Therefore, the analytical model proposed by Hsiao et al. [11] was adopted, which is characterized by a combination of a nonlinear rotational spring located at the physical end of the brace and several rigid elements that represent regional enhanced stiffness, as shown in Figure 9b. Figure 9c shows the center part where four brace diagonals are connected by the gusset plate. The FE model adopts a similar approach by linking four nonlinear rotational springs with rigid elements intersecting at the centroid of the middle gusset plate.

3.2.2 Model validation

Validation of the numerical model of the double-angle L-shaped bracing strut intends to reproduce the hysteretic performance of specimen strut 8 tested under cyclic loading by Black et al. [13]. The simulated hysteretic response of the brace against the experimental data is presented in Figure 10. Considerable deterioration of strength and stiffness under compression is shown if compared to the stable performance in tension.

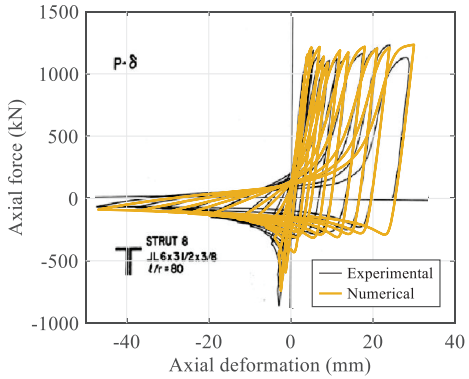

Figure 10: Validated hysteretic response of double-angle brace

https://doi.org/10.52202/069179-0423

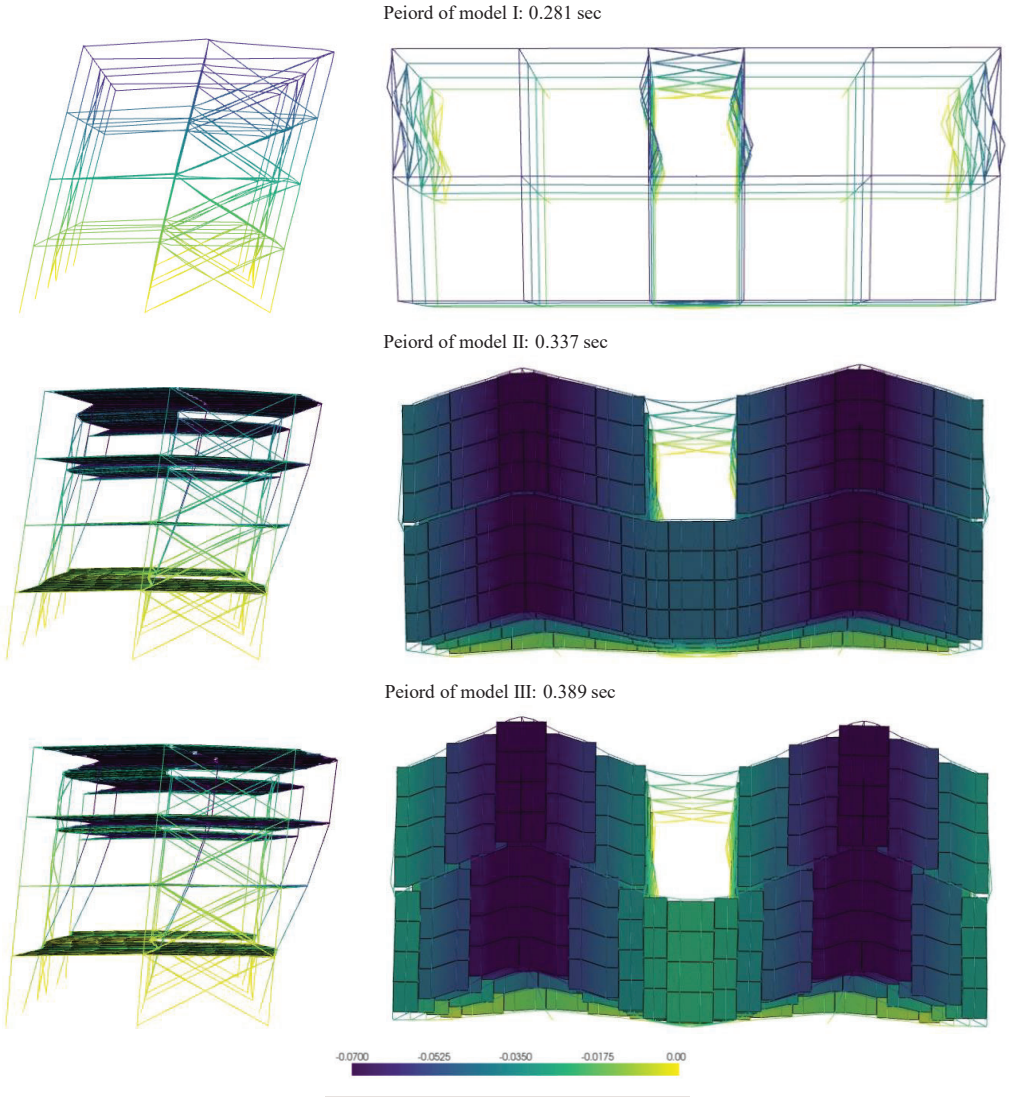

Figure 11: Mode shape 2 (translation in the south-north direction) of three building models

Three FE models of the building were analyzed. The building model with fully rigid floor diaphragms is denoted as Model I. With the hybrid CLT-steel floor system and panel-to-panel connections the building model is denoted as Model II. The companion model without the panel-to-panel connections is denoted as Model III.

4 MODAL RESPONSE

Table 2: Periods (sec) of first three mode shapes

Model	Mode 1	Mode 2	Mode 3
I	0.408	0.281	0.242
II	0.454	0.337	0.312
III	0.571	0.389	0.384

Modal analysis was conducted to calculate periods of the first three mode shapes: horizontal translation in the east-west direction, horizontal translation in the south-north direction, and torsion, as shown in Table 2. Figure 11 depicts the translational mode shape 2 of three building models. Specifically, the first two periods of Model II are both about 0.05 s longer than those of Model I. In case of hybrid CLT diaphragms without the panel-to-panel STS connections, the model has 40% higher periods, if compared to Model I, regarding the two translational mode shapes. For torsion, Model III has a period of 0.384 s and that is approximately 60% higher than that of Model I. It can be noted that the reinforcement of STSs between CLT panels conspicuously reduces the overall in-plane flexibility of diaphragms. Besides, the lack of restraints between CLT panels underpins the aggregated behaviour of in-plane shear deformation and rotation of individual

https://doi.org/10.52202/069179-0423

hybrid floor modules, which conceivably elongates the translational and torsional periods of the building archetype.

5 FRAGILITY ANALYSES

To retrieve a comprehensive evaluation of the seismic performance of different building models through IDA, a total of 20 ground motion records were selected from the Pacific Earthquake Engineering Research Center Shallow Crustal Earthquakes database [14], scaled to a minimum mean square error with respect to the target spectrum over a period range from 0 seconds to 2.5 seconds, which is determined by the period of dominance according to the local disaggregation results retrieved from the software REXEL [15] for site Bucchianico, Chieti, Italy. Figure 12 plots the uniform hazard spectrum, which corresponds to a hazard level of 10% probability of occurrence in 50 years, and the selected records.

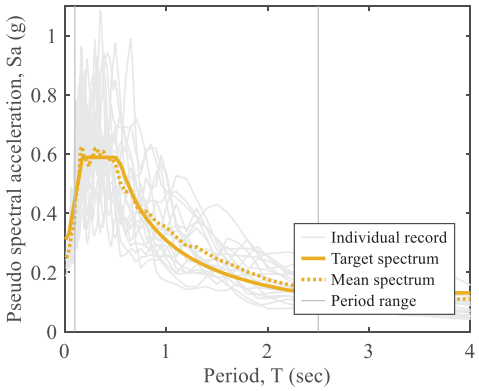

***Figure 12**: Target response spectrum and selected records*

Three damage states (DSs) are of interest when evaluating their exceeding likelihoods given a certain level of ground shaking intensity, as expressed by a cumulative distribution function and plotted by a fragility curve. Particularly, DS1 identifies the transition point between the model's elastic behaviour and the first nonlinearity. DS2 refers to a 2% maximum inter-story drift ratio (ISD), which is associated with the collapse prevention performance level for braced steel frames specified in FEMA 356 [16]. In addition, DS3 is determined by either the simulated collapse point, where a single IDA curve reaches a plateau due to deteriorating mechanisms or the last converged time-integration step.

Figure 13 shows the probability of exceeding different DSs as a function of the intensity measure (IM), which is represented by the 5%-damped spectral acceleration at the structure's fundamental period Sa (T_1, 5%).

By comparing three fractiles of IM, Model II has the highest spectral acceleration to exceed DS1. To be specific, 16% of records need to reach Sa $\geq$ 0.95g, 50% of records need to reach Sa $\geq$ 1.27g, and 84% of records need to reach Sa $\geq$ 1.70g. This suggests that implementation of the proposed hybrid CLT diaphragm enables the building to sustain a median intensity of ground motion up to approximately two times the intensity of the design uniform hazard (i.e., 0.59g), before any structural nonlinearity arises. The median Sa of Model II is 0.1g and 0.18g greater than those of Model I and III.

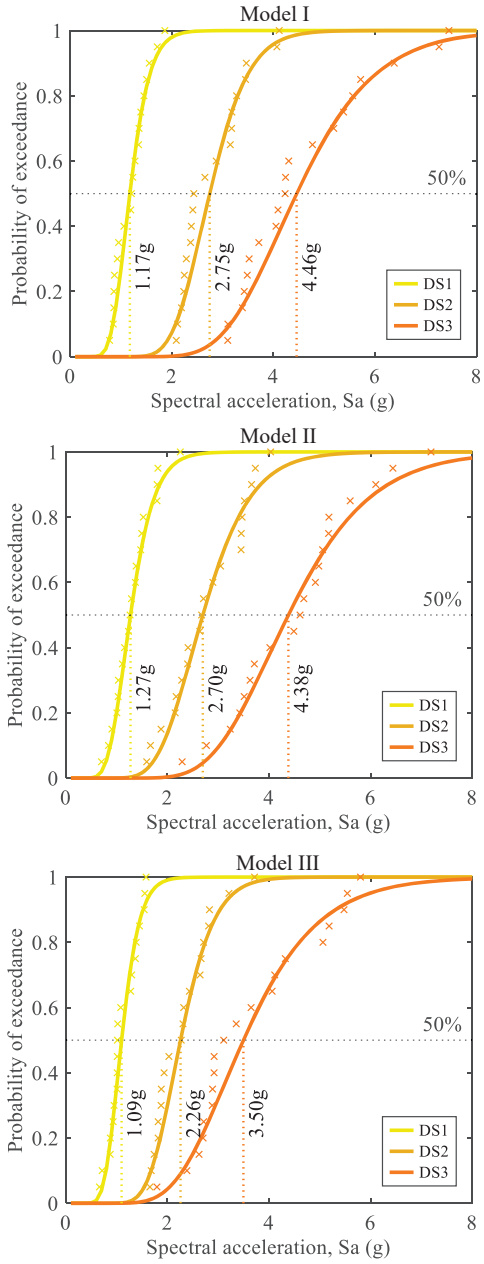

***Figure 13:** Fragility curves under three damage states*

In case of exceeding DS2, the 16% Sa capacity of Model I is approximately 8% and 23% higher than that of Models II and III. A trivial difference is observed in the median value between Model I and Model II. The intensity value at which 84% of the records need to be scaled to produce the demand δ = 2% is 3.54 g for Model II, which is significantly higher than the value of Model III, while

https://doi.org/10.52202/069179-0423

close to that of Model I. A similar trend was found concerning the global collapse limit state; and no major difference was observed in all three fractiles of IM between Models I and II. Compared to Model III, however, Model II has a 25% (i.e., 4.38 g) and 21% (i.e., 5.84 g) larger value at the 50% and 84% percentile, respectively. Consequently, it can be summarized that the required intensity for Model I and Model II to exceed DS2 and DS3 are comparatively similar; and that shaking level needs to be reduced by more than 20% for Model III to reach both DSs.

6 CONCLUSIONS

The seismic fragilities of an innovative mass timber-steel hybrid building archetype equipped with prefabricated CLT-steel composite floor diaphragms were presented. The 3D numerical model developed in OpenSees entailed critical nonlinearities primarily contributed by deteriorating behaviours of steel structs, such as the low cycle fatigue behaviour and section fracture mechanism of the bracing member. Particularly, the local failure modes were incorporated explicitly into the calibrated sub-models of the CLT-steel floor diaphragms, including the beam-to-beam connections. Building archetype assembled by the validated sub-models was subjected to the incremental dynamic analysis, assuming a suite of 20 ground motion records that were scaled up to the global collapse of the building. The building's seismic performance was assessed using fragility curves. Based on the probabilistic analysis results, it can be concluded that the overall seismic performance of Model II is comparatively similar to that of Model I in terms of the conditional probability of exceeding all three damage states, given any level of ground motion intensity. In the context of adopting the proposed CLT-steel floor diaphragm module, careful considerations should be placed on the panel-to-panel connections, as they are contributors to the overall in-plane stiffness of floor subassemblies.

ACKNOWLEDGEMENT

This research was financed by the Natural Sciences and Engineering Research Council (NSERC) of Canada through the Discover Program, grant number RGPIN-2019-04530, and Discovery Launch Supplement, grant number DGECR-2019-00265. The Donald S. McPhee Fellowship and Robert and Averil Kennedy Wood Science Graduate Scholarship awarded to Chaoyue Zhang are also acknowledged. Free access to the Digital Research Alliance of Canada computer cluster is also acknowledged (https://alliancecan.ca/en).

REFERENCES

[1] J. Humar and M. Popovski, "Seismic response of single-storey buildings with flexible diaphragms," *Can. J. Civ. Eng.*, vol. 40, no. 9, pp. 875–886, 2013, doi: 10.1139/cjce-2012-0493.

[2] A. Roncari, F. Gobbi, and C. Loss, "Nonlinear static seismic response of steel frame buildings equipped with hybrid cross-laminated timber floor diaphragms," *Front. Built Environ.*, 2020.

[3] Italian Ministry of Infrastructure and Transport, "Istruzioni per l'applicazione delle «Nuove norme tecniche per le costruzioni» di cui al decreto ministeriale 14 gennaio 2008," *Gazzetta Ufficiale della Repubblica italiana*, 2009.

[4] C. Eurocode, "8: Design of structures for earthquake resistance—Part 1: General rules, seismic actions and rules for buildings (EN 1998-1: 2004)," *Eur. Comm. Norm. Brussels*, 2004.

[5] C. Loss and A. Frangi, "Experimental investigation on in-plane stiffness and strength of innovative steel-timber hybrid floor diaphragms," *Eng. Struct.*, 2017, doi: 10.1016/j.engstruct.2017.02.032.

[6] F. McKenna, M. H. Scott, and G. L. Fenves, "Nonlinear Finite-Element Analysis Software Architecture Using Object Composition," *J. Comput. Civ. Eng.*, vol. 24, no. 1, pp. 95–107, 2010, doi: 10.1061/(asce)cp.1943-5487.0000002.

[7] C. Loss, M. Piazza, and R. Zandonini, "Connections for steel–timber hybrid prefabricated buildings. Part II: Innovative modular structures," *Constr. Build. Mater.*, 2016, doi: 10.1016/j.conbuildmat.2015.12.001.

[8] M. H. Scott, G. L. Fenves, F. McKenna, and F. C. Filippou, "Software Patterns for Nonlinear Beam-Column Models," *J. Struct. Eng.*, vol. 134, no. 4, pp. 562–571, 2008, doi: 10.1061/(asce)0733-9445(2008)134:4(562).

[9] P. Uriz, F. C. Filippou, and S. A. Mahin, "Model for Cyclic Inelastic Buckling of Steel Braces," *J. Struct. Eng.*, vol. 134, no. 4, pp. 619–628, 2008, doi: 10.1061/(asce)0733-9445(2008)134:4(619).

[10] M. H. Scott and F. C. Filippou, "Response Gradients for Nonlinear Beam-Column Elements under Large Displacements," *J. Struct. Eng.*, vol. 133, no. 2, pp. 155–165, 2007, doi: 10.1061/(asce)0733-9445(2007)133:2(155).

[11] P. C. Hsiao, D. E. Lehman, and C. W. Roeder, "Improved analytical model for special concentrically braced frames," *J. Constr. Steel Res.*, vol. 73, pp. 80–94, 2012, doi: 10.1016/j.jcsr.2012.01.010.

[12] J. H. Yoo, "Analytical Investigation on the Seismic Performance of Special Concentrically Braced Frames," 2006.

[13] G. Black, W. A. B. Wenger, and E. P. Popov, "Inelastic Buckling of Steel Struts Under Cyclic Load Reversals," Berkeley, CA, 1980.

[14] "PEER Ground Motion Database - PEER Center." https://ngawest2.berkeley.edu/ (accessed Feb. 20, 2023).

[15] I. Iervolino, C. Galasso, and E. Cosenza, "REXEL: Computer aided record selection for code-based seismic structural analysis," *Bull. Earthq. Eng.*, 2010, doi: 10.1007/s10518-009-9146-1.

[16] ASCE, "American Society of Civil Engineers, FEMA 356 Prestandard and Commentary for the Seismic Rehabilitation of Building," *Rehabilitation*, no. November, 2000.

https://doi.org/10.52202/069179-0423